Advanced Ceramics Progress: Vol. 8, No. 2, (Spring 2022) 1-11

Materials and Energy Research Center
MERC

Contents lists available at ACERP

Advanced Ceramics Progress

Journal Homepage: www.acerp.ir

Original Research Article

Oxidation Behavior of HfB_2-SiC-Nd_2O_3 Ultra-High Temperature Composite Sintered through SPS Process

Younes Hanifeh [a], Maryam Shojaie-Bahaabad [b,*], Mohammad Jafar Molaei [b]

[a] *MSc Student, Faculty of Chemical and Materials Engineering, Shahrood University of Technology, Shahrood, Semnan, Iran*
[b] *Assistant Professor, Faculty of Chemical and Materials Engineering, Shahrood University of Technology, Shahrood, Semnan, Iran*

* Corresponding Author Email: mshojaieb@shahroodut.ac.ir (M. Shojaie-Bahaabad)

URL: https://www.acerp.ir/article_149762.html

ARTICLE INFO

Article History:

Received 6 April 2022
Received in revised form 8 May 2022
Accepted 14 May 2022

Keywords:

HfB_2-SiC-Nd_2O_3 Composite
Oxidation Behavior
Spark Plasma Sintering
Rare Earth Element

ABSTRACT

The current study aims to fabricate HfB_2-30 vol. % SiC and HfB_2-30 vol. % SiC-2 vol. % Nd_2O_3 composites through Spark Plasma Sintering (SPS) method at 1950 °C for 10 min. The oxidation behavior of the prepared composites was investigated at 1400 °C and different times namely 4, 8, 12, and 16 hours. The relative density, hardness, toughness, and strength of the HfB_2-30 vol. % SiC composite increased from 98.5 %, 20.19 GPa, 414.9 MPa, and 4.36 MPa.$m^{0.5}$ up to 99.1 % , 24.47 GPa, 485 .5 MPa, and 4.93MPa.$m^{0.5}$ for HfB_2-30 vol. % SiC-2 vol. % Nd_2O_3 composite, respectively. After 16 hours of oxidation, SiO_2 layer, which was extremely thick, was produced locally on the oxidized HfB_2-30 vol. % SiC composite surface. The thinckness of the SiO_2 layer was calculated to be around 25 µm. The thickness measurement revealed the SiO_2 produced layer on the surface of the HfB_2-30 vol. % SiC-2 vol. % Nd_2O_3 composite to be 5 µm. The oxidation kinetic results of the composite exhibited linear-parabolic behavior. The chemical reaction during the oxidation process controlled the oxidation rate after eight hours. After 16 hours of performing the oxidation procedure at 1400 °C, HfB_2-30 vol. % SiC-2 vol. % Nd_2O_3 composite exhibited parabolic behavior, while HfB_2-30 SiC exhibited linear behavior. This composite's improved oxidation resistance was attributed to $Nd(Hf,Si)O_xC_y$ phases and decreased porosity, resulting in the generation of thin, dense, adherent, and protective layers. Therefore, it was concluded that the oxygen diffusion rate could control the oxidation process in HfB_2-30 vol. % SiC-2 vol. % Nd_2O_3 composite.

https://doi.org/10.30501/acp.2022.336283.1086

1. INTRODUCTION

Ceramic materials characterized by high melting temperatures (> 3000 °C) are referred to as Ultra-High Temperature Ceramics (UHTCs) that are promising materials for Thermal Protection Systems (TPSs). Transition metal nitrides, carbides, and diborides are known as the members of the UHTCs family [1-3]. These compounds have such characteristics as high melting point, good thermal and electrical conductivity, excellent stability against metal melt, considerable heat shock resistance, high Young's modulus, and relatively good hardness and resistance against chemical attacks [4]. Of note, higher melting point (e.g., 3380 °C) and better electrical and thermal conductivity of HfB_2 than those of other intermetallic compounds such as carbides, nitrides, and deborides have encouraged researchers to shift their focus to conducting extensive research on HfB_2-based ceramics [5,6].

HfB_2 ceramics are commonly fabricated through

Please cite this article as: Hanifeh, Y., Shojaie-Bahaabad, M., Molaei, M. J., "Oxidation Behavior of HfB_2-SiC-Nd_2O_3 Ultra-High Temperature Composite Sintered through SPS Process", ***Advanced Ceramics Progress***, Vol. 8, No. 2, (2022), 1-11. https://doi.org/10.30501/acp.2022.336283.1086

pressureless sintering (> 2150 °C), hot pressing (1800-2000 °C), and Spark Plasma Sintering (SPS) methods. Without using sintering aids, HfB_2 ceramics are densified at temperatures above 2000 °C in the range of 20-30 MPa and at a temperature of about 1700-1800 °C in the range of 800-1500 MPa as well through hot pressing [7-10]. SPS is a favorable process used to compact HfB_2 ceramics at lower temperatures in a short time period that needs less sintering aid than the conventional methods.

In recent years, several researchers have employed the SPS method for HfB_2 ceramics compaction. This method applies direct pulse current and external axial force in a simultaneous manner on compacted powder in a graphite die in order to accelerate sintering. Its high heating rate and low sintering temperature, compared to other methods, yield a finer microstructure. Owing to the spark created among the powder particles and use of direct pulse flow, this method can successfully compact materials with poor sinterability [11-14]. Moreover, additives such as metals, nitrides, carbides, and desilicides are usually used for improving the sintering consolidation of HfB_2 ceramics [15-19].

One of the main drawbacks of HfB_2 ceramics is, however, their poor oxidation resistance. HfB_2 oxidation begins at the low temperature of about 1000 °C, depending on the oxygen partial pressure. The molten B_2O_3 fills the pores, thus forming a protective layer to prevent further oxidation of matrix up to the temperature of 1100 °C. At a temperature of about 1400 °C, upon increasing the oxygen partial pressure, B_2O_3 and HfB_2 are rapidly evaporated and oxidized, respectively, hence formation of some porous and cracked layers on the surface [20].

A promising approach to improving the oxidation resistance of HfB_2 ceramics is the addition of SiC to HfB_2, typically in the volume range of 10-30 vol. %. Followed by oxidization of HfB_2-SiC composite, a borosilicate glassy layer is developed on the composite surface. The borosilicate layer melts at a lower temperature, yet it can withstand temperatures up to 2000 °C for about 1 h in a non-air flowing atmosphere [20]. The borosilicate layer vanishes at termperatures above 2000 °C and the bulk composite is likely to experience active oxidation.

A variety of methods have been proposed to date to improve the oxidation resistance of UHTC HfB_2-SiC ceramics, some of which are listed in the following: adding different compounds such as Si and making a solid solution using HfB_2 [14,21-23], increasing the viscosity and melting point of the borosilicate layer by adding metal elements [24], adding metal boride compounds [25-27], using rare earth compounds, and forming refractory phases with a high melting temperature in the protective layer [28,29], to name a few. There are, however, few studies that already investigated the long-term oxidation of HfB_2-SiC coating at a temperature of 1500 °C for 50 [30] and 753 h [31]. Studies on the oxidation are commonly conducted at tempratures of 1500-1700 °C up to 10 h [21,24]. Zapata-Solvas et al. reported the oxidation kinetics for the HfB_2-SiC-La_2O_3 composite in the temprature range of 1400-1600 °C for up to 32 h [32]. In the particular case of adding Nd_2O_3, $Nd_2Hf_2O_7$ pyrochlore compound has a low vapor pressure at high temperatures (> 2000 °C) [33]. In addition to the phase stability in such a wide temperature range, the melting point of neodymium hafinate is high (2330-2700 °C), as reported in many studies [34]. As a result, it makes this crystal phase a good candidate for UHTCs which needs to withstand the temperatures of about 2000 °C.

However, almost no study has been conducted on the oxidation behavior of HfB_2-SiC-Nd_2O_3 composites. In this regard, the current study aimed to fabricate HfB_2-30 vol. % SiC-2 vol. % Nd_2O_3 composite through the SPS method. In fact, this research makes a comparison between the prepared composite and HfB_2-30 vol. % SiC composite in terms of their oxidation resistance. The oxidation behavior of the obtained composites was also examined at a temperature of 1400 °C and different times of 4, 8, 12, and 16 h.

2. MATERIALS AND METHODS

Commercial HfB_2 (Beijing Cerametek Materials Co., China, particle size of < 2 µm and purity of > 99 %), SiC (Xuzhou Co., China, particle size of < 10 µm and purity of 99 %), and Nd_2O_3 (Xuzhou Co., China, particle size of < 5 µm and purity of 99.8 %) powders were used and mixed to make HfB_2-30 vol. % SiC-Nd_2O_3 composites. The theoretical densification values for SiC, HfB_2, and Nd_2O_3 were obtained as 3.2 g/cm^3 for, 11.2 g/cm^3, and 7.24 g/cm^3, respectively, and the volume fractions of the raw materials were calculated based on these values to achieve the final compositions. The powder mixtures were minced through high-energy planetary milling using balls and a WC-Co cup at 300 rpm for three hours in ethanol medium at the weight ball to powder ratio of 10:1. The slurry was then dried out at a temperature of 60 °C for two hours. HfB_2-30 vol. % SiC composites containing 0 and 2 vol. % Nd_2O_3 (named Nd0 and Nd2) were prepared through the SPS method at 1950 °C in 10 min with the vacuum of 0.05 mbar under the pressure of 40 MPa. The relative densification in the distilled water was then calculated using Archimedes technique; theoretical densification was measured based on the mixtures' law. Phase analysis of the composites was performed by the X-ray diffraction pattern (XRD, Philips, Model: X'Pert MPD, Co Kα1, λ: 1.78897 Å); their surface and microstructure were studied using Field Emission Scanning Electron Microscope (FESEM, TESCAN, Model: MIRA) prepared by Energy Dispersive Spectroscopy (EDS). The hardness of the composites was then measured by utilizing the Vickers hardness tester under 1 kg, with the loading time being 10 s. The toughness of composites was obtained using

Equation 1 [28]:

$$K_{IC} = 0.073 (P/c^{1.5}) \quad (1)$$

where K_{IC} represents the fracture toughness (MPa.$m^{1/2}$), P the applied load (N), and c the average half-length of the crack (µm). The flexural strength of composite was evaluated using a three-point flexural machine (Zwick Roell SP600, Germany) having a loading rate of 0.05 mm/min. Oxidation behavior was investigated in an electric furnace at a temperature of 1400 °C for 4, 8, 12, and 16 h. The oxidation resistance of composites was then evaluated based on the weight changes and the oxide layer thickness following oxidation.

3. RESULTS AND DISCUSSION

The densification of the prepared composites exhibited that by adding Nd_2O_3 up to 2 vol. %, composite densification was enhanced from 98.5 % to 99.1 %. Nd_2O_3 seemed to react with oxide impurity on the surface of HfB_2 and SiC particles, forming a liquid phase, as a result of which powders sinterability and densification were increased [29,33].

The XRD patterns of the composites following the SPS process are shown in Figure 1. Based on the XRD patterns of the composites, HfB_2 and SiC phases could be seen in the samples, too. The trace of $Nd_2Hf_2O_7$ phase was identified in the Nd2 composite. Thus, HfO_2 impurities on the surface of HfB_2 particles reacted, leading to the formation of Nd_2O_3 and $Nd_2Hf_2O_7$ phase [35].

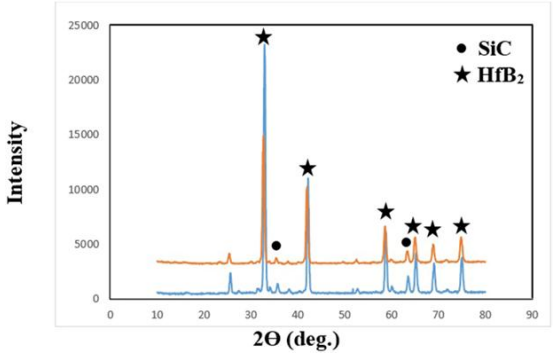

Figure 1. XRD patterns of the sintered composites

Figure 2 shows the SEM image and EDS analysis of the composite surface following the SPS process. Based on the EDS analysis, the dark and light gray areas were SiC and HfB_2 phases, respectively. At the junction of several HfB_2 grains, dark gray areas could be observed. According to the XRD patterns and EDS analysis (Figure 1 (C)), these areas were $Nd_2Hf_2O_7$.

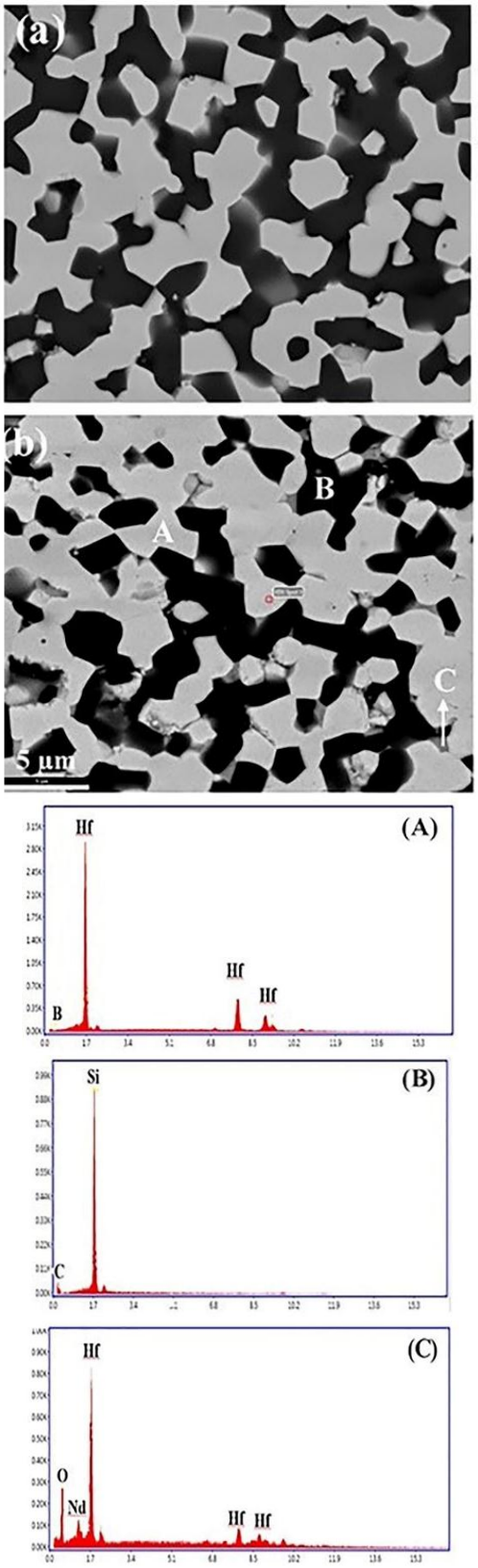

Figure 2. FESEM images and EDS analysis of the sintered composites: (a) HfB_2-SiC and (b) HfB_2-SiC-2 vol. % Nd_2O_3

Figure 3 shows the sintered composites' fracture surface. An oxide layer on the surfaces of non-oxide particles (e.g., SiO_2 B_2O_3, and HfO_2) led to the generation of borosilicate glassy phases. Jaberi et al. investigated the ZrB_2-SiC composite prepared by the hot pressing method and found that the glassy phase in the SEM images appread in the form of a cleavage or planar state, thin thickness, or inelastic and elastic fracture surface [36]. Such a glassy phase was well visible in the SEM images obtained from the cross-section of the composites that had been prepared in the present research (dashed flash). The HfB_2-SiC composites had an intergranular-transgranular fracture. Particles pullout and sharp edges could be seen in the photos, thus implying that the intergranular fracture had happened across the grain boundary (thick arrows). Elastic and broad surfaces reflecting transgranular fractures could be detected in some regions (narrow arrows), particularly when confronted with atypical grain growth, in comparison to others.

The investigation of the mechanical properties of thHfB_2-30 SiC composite demonstrated that the hardness, flexural strength, and toughness of the Nd0 specimen were 20.19 GPa, 414.9 MPa, and 4.36 MPa.$m^{0.5}$. When the addition of Nd_2O_3 to the HfB_2-30 SiC composite was done, the hardness, flexural strength, and toughness of the composites increased to 24.47 GPa, 485 .5 MPa, and 4.93MPa.$m^{0.5}$, respectively, because of the rise of the densification of the composite. Researchers have also investigated the impact of Re_2O_3 addition on the mechanical properties of ZrB_2-based composites [37]. They reported the improved densification of ZrB_2-SiC composites which were doped with Re_2O_3 due to the ability of Re_2O_3 to form liquid phases with SiO_2, B_2O_3, and ZrO_2 impurities, thus strengthening the grain boundaries. So, stronger grain boundaries and denser matrix with lower residual porosity could enhance mechanical properties. In the present research study, similar results were obtained in regard to HfB_2-SiC-Nd_2O_3 composite.

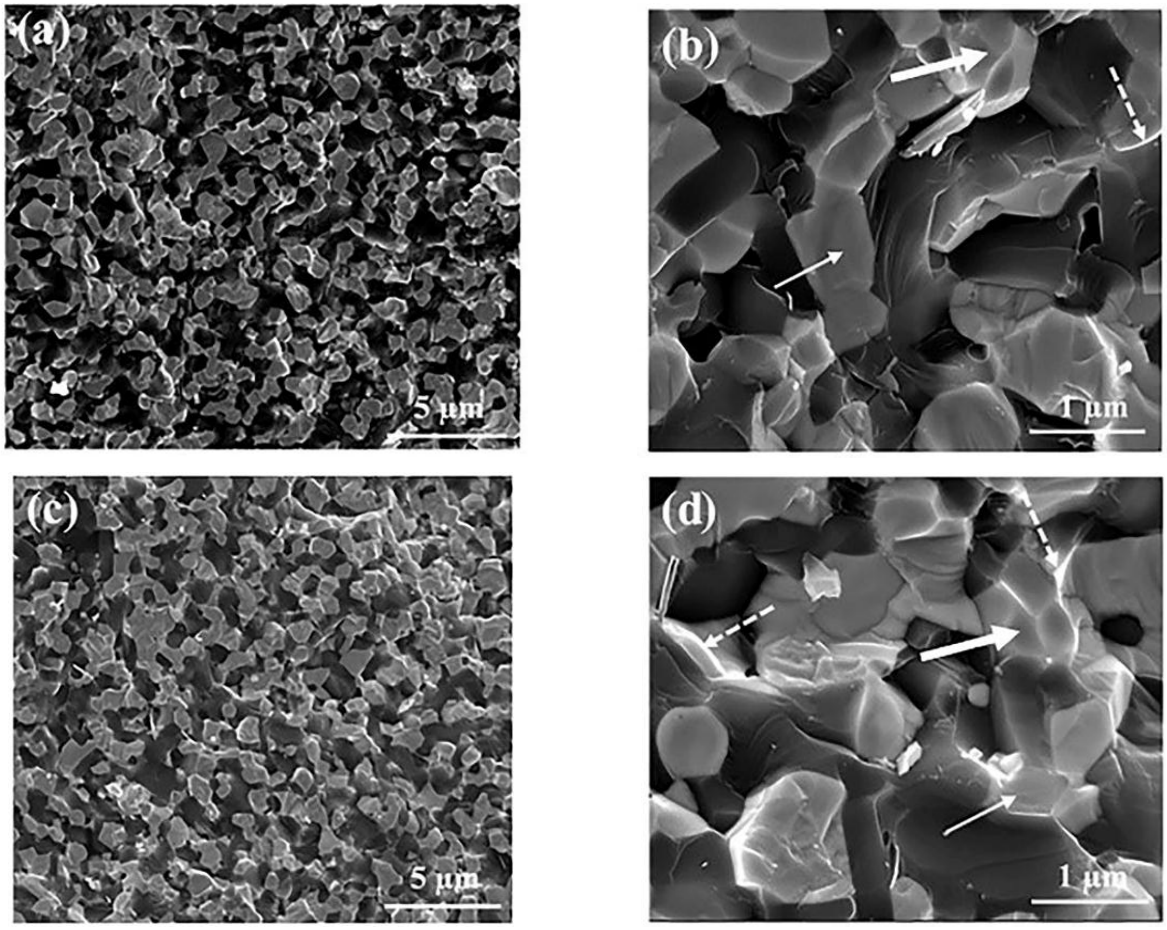

Figure 3. FESEM images of the fracture surface of the sintered composites: (a,b) HfB_2-SiC and (c,d) HfB_2-SiC-2 vol. % Nd_2O_3

The effects of the Vickers hardness indenter on HfB_2-30 SiC composites are depicted in Figure 4. As shown in the Nd2 sample, the hardness test had a regular effect and no deformation was observed around it. This could be due to the high densification of this sample, as compared to the Nd0 sample. In the Nd0 sample, the hardness effect

was more irregular due to the higher porosity of this composite.

XRD patterns of HfB_2-SiC composites, following oxidation at a temperature of 1400 °C for 16 h, are shown in Figure 5. In HfB_2-SiC composites, $HfSiO_4$ and HfO_2 phases could be seen as the main phases and some SiO_2 phase was identified in the XRD patterns following oxidation.

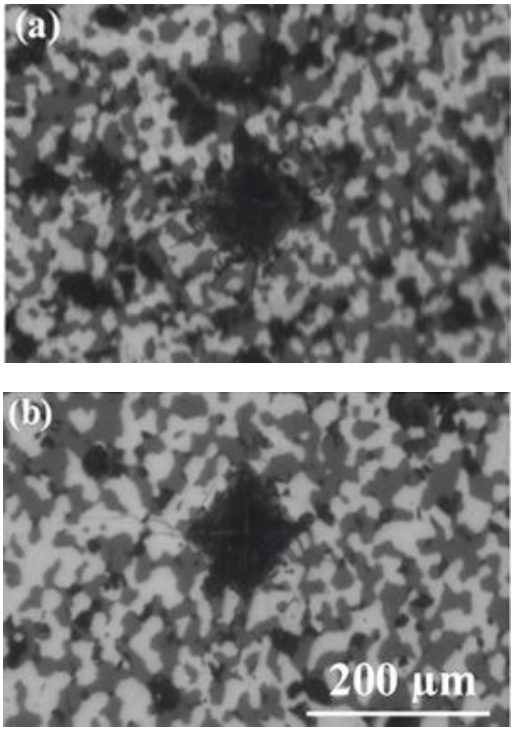

Figure 4. FESEM images of Vickers indenter effect of the sintered composites: (a) HfB_2-SiC and (b) HfB_2-SiC-2 vol. % Nd_2O_3

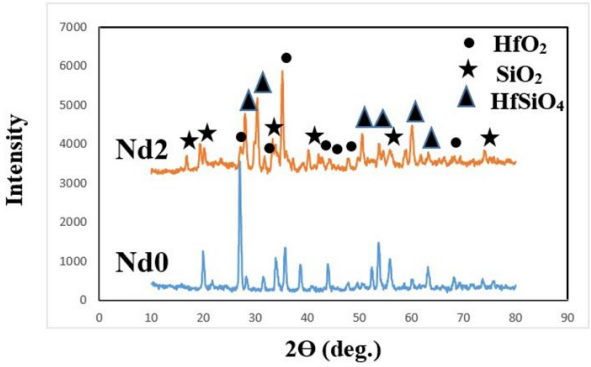

Figure 5. XRD patterns of the sintered composites after the oxidation test at 1400 °C for 16 h

The HfB_2-30 SiC composite surface following oxidization at a temperature of 1400 °C for different times is shown in Figure 6. The composite's surface was locally coated with a glass layer and evenly distributed on the composite surface following oxidation for a period of 16 h.

Oxidation of SiC particles at temperatures above 1100 °C led to the generation of some SiO_2 glass layer on the composite surface [38]. EDS analysis also showed that the glass layer was evenly composed of Si and O. Further, the white crystals with different sizes and shapes were observed on the composites surafce following oxidation. According to the EDS analysis, spherical crystals with Hf and O high content were HfO_2 crystals. The surface of the Nd2 composite was smoothly coated by this oxide layer; it consisted of a needle-like crystal phase following oxidation for more than 12 h.

According to the EDS analysis (Figure 7), these crystals with equal Hf and Si content were $HfSiO_4$ crystals. The formation of crystalline phases in the present study is described in the following. Following the formation of SiO_2 and HfO_2 and molten B_2O_3 (according to reactions (2) and (3)) [36], there was the dissolution of HfO_2 in borosilicate melt first, leading to the formation of SiO_2-B_2O_3 (HSB) liquid in the glass layer.

$$2\ SiC\ (s) + 3\ O_2\ (g) = 2\ SiO_2\ (l) + 2\ CO\ (g) \quad (2)$$

$$2\ HfB_2\ (s) + 5\ O_2\ (g) = 2\ HfO_2\ (s) + 2\ B_2O_3\ (l) \quad (3)$$

Then, with the development of the oxidation process, the HSB liquid flowed on the top of the glass layer. Upon evaporation of B_2O_3, precipitation of HfO_2 particles from the HSB liquid occurred. Further, HfO_2 could react with SiO_2 (reaction (4)) and $HfSiO_4$ particles could also be formed [35].

$$SiO_2\ (l) + HfO_2\ (s) = HfSiO_4\ (s) \quad (4)$$

The molten B_2O_3 evaporates at temperatures above 1100 °C; its evaporation rate is faster than the formation rate of the molten B_2O_3 in the temperature range of 1100-1400 °C, according to Reaction (5) [39]. Thus, B_2O_3 phase was not observed in the X-ray pattern of composites following oxidation.

$$B_2O_3\ (l) = B_2O_3\ (g) \quad (5)$$

As can be seen in the XRD patterns, the trace $HfSiO_4$ phase was also formed in the Nd0 sample. As mentioned before, SiO_2 was locally distributed on the surface of Nd0 composite. As a result, $HfSiO_4$ particles were formed in lower amounts, as compared locally to the Nd2 composite. Based on the formation of $HfSiO_4$ silicate phase and the locking effect of this phase in the glassy layer, the oxide layer which was formed on the surafce of the Nd2 sample protected the HfB_2-30 SiC composite in a more effective manner than the Nd0 composite.

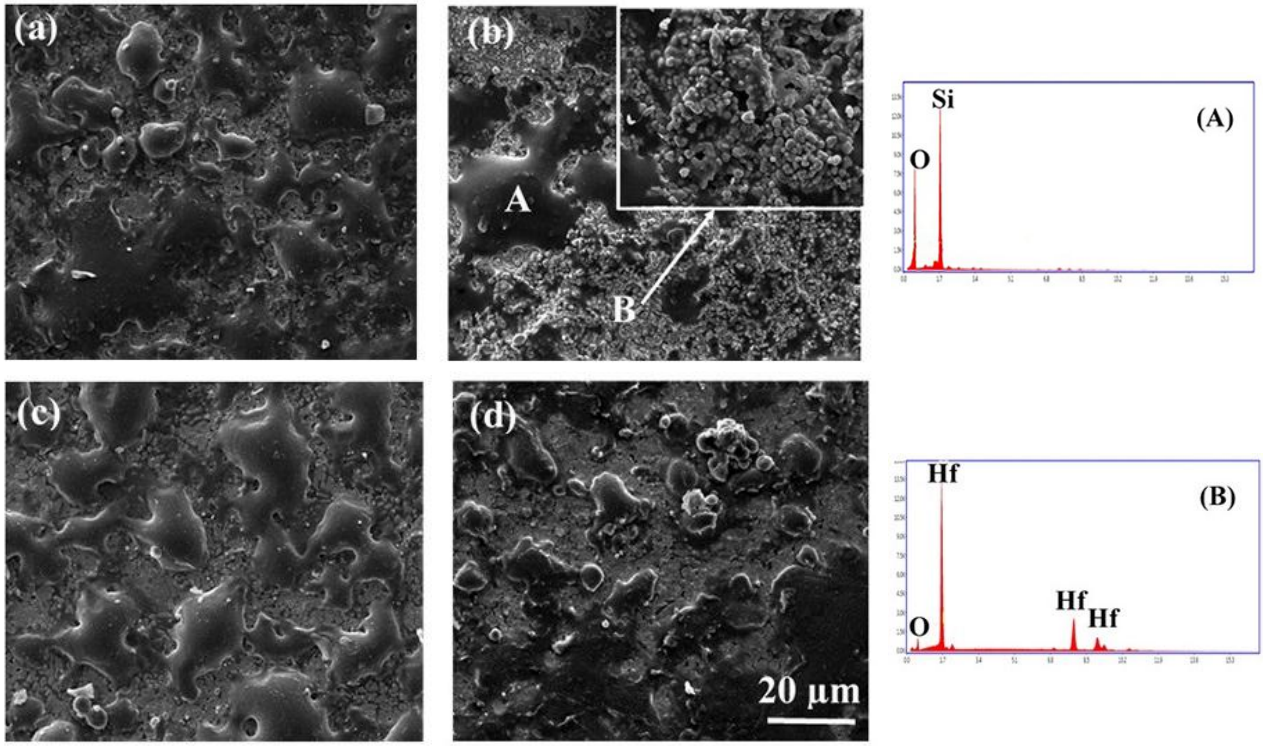

Figure 6. FESEM image and EDS analysis of the surface of HfB_2-SiC composite after the oxidation test at 1400 °C at different times: (a) 4, (b) 8, (c) 12, and (d) 16 h

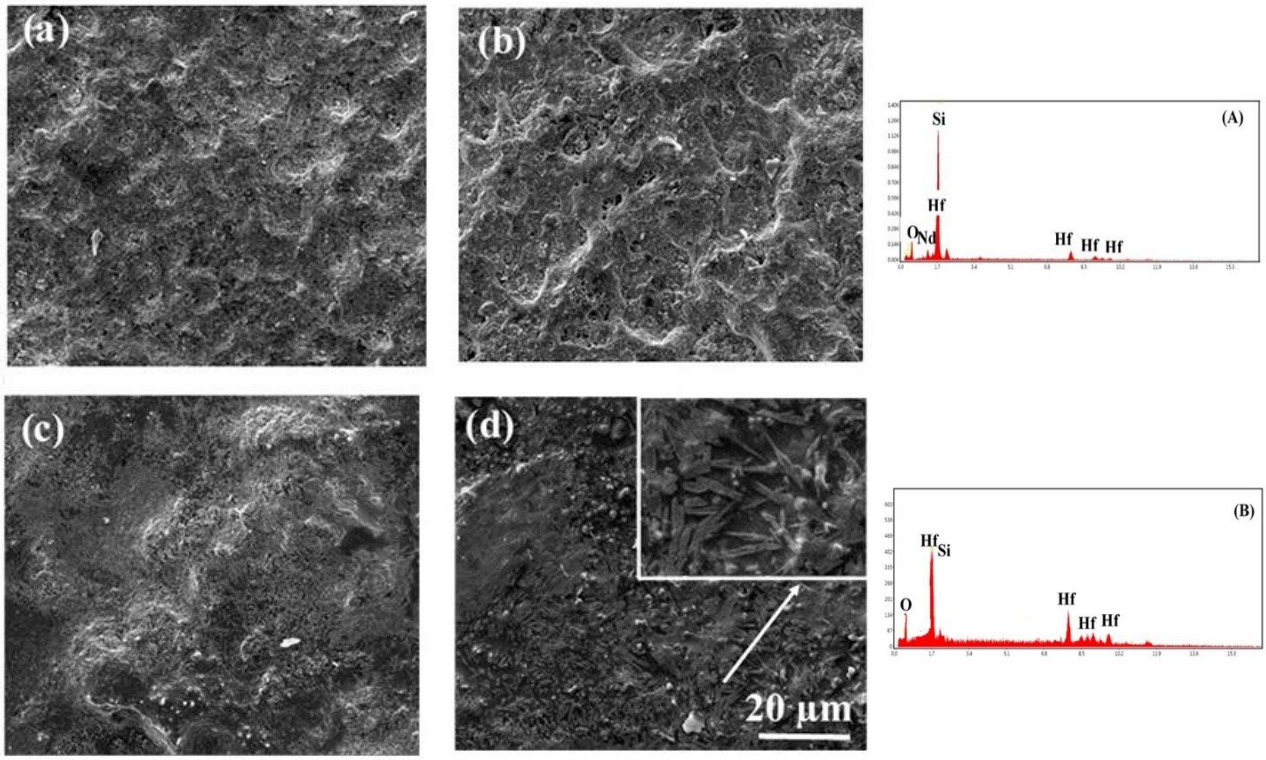

Figure 7. FESEM image and EDS analysis of the surface of HfB_2-SiC-2 vol. % Nd_2O_3 composite after the oxidation test at 1400 °C for different times, (a) 4, (b) 8, (c) 12, and (d) 16 h

Figures 8 and 9 represent the composites' sample cross-section following the oxidation test for different times. According to the EDS analysis, the first layer was rich in Si and the second one had moderate values of Si and Hf.

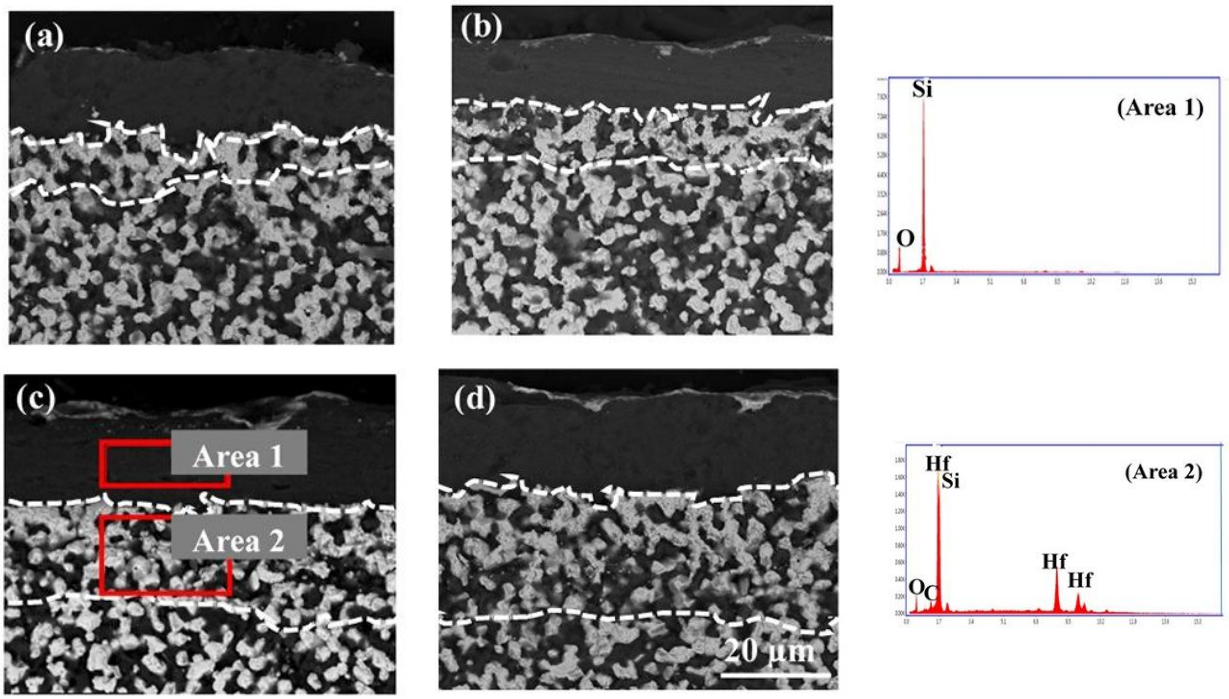

Figure 8. FESEM image and EDS analysis of cross-section of HfB_2-SiC composite after the oxidation test at 1400 °C for different times, (a) 4, (b) 8, (c) 12, and (d) 16 h

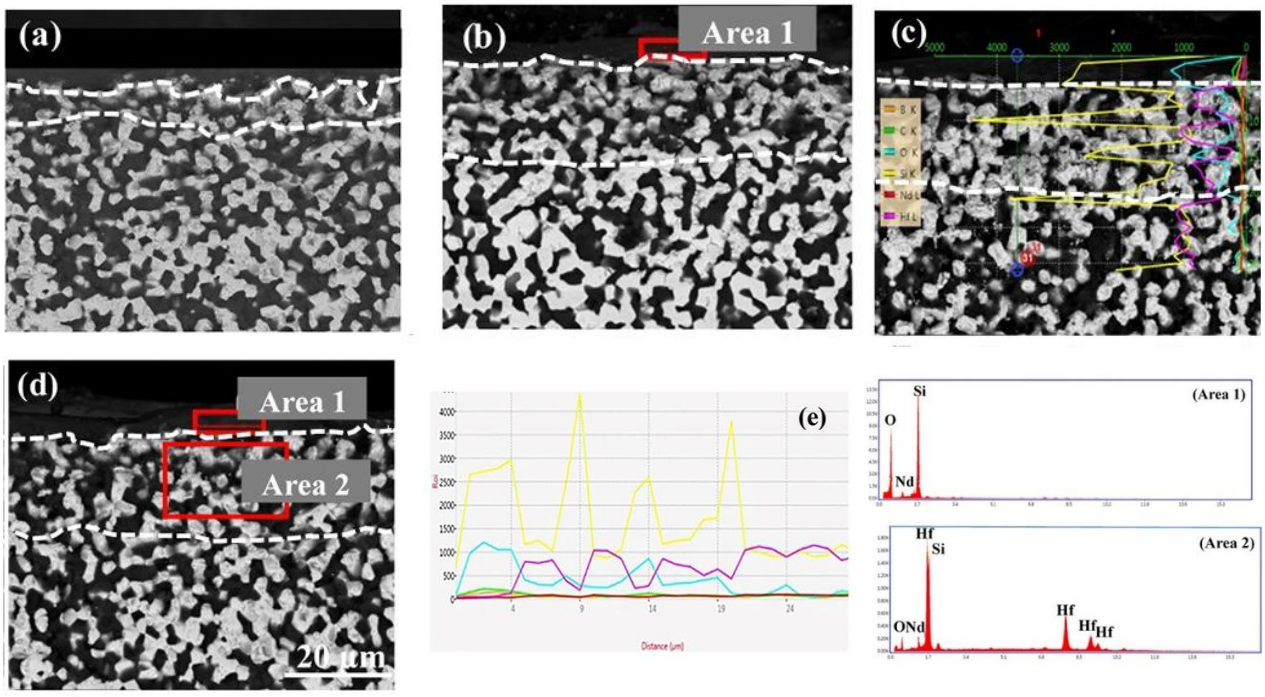

Figure 9. FESEM image and EDS analysis of cross-section of HfB_2-SiC-2 vol. % Nd_2O_3 composite after the oxidation test at 1400 °C for different times, (a) 4, (b) 8, (c) 12, and (d) 16 h

The thickness of the SiO_2 rich layer which was produced on HfB_2-30 SiC composites' surface following the oxidation test can be seen in Figure 8. As can be observed, the overall oxide layer thickness was increased greatly with increasing the duration time for the HfB_2-30 SiC composite. The SiO_2 oxide layer was not smoothly formed on the surface during oxidation. Over time, a partial glass layer and greater porosity might enhance oxygen penetration into the bulk. Because of the growth of the oxide scale layer throughout the oxidation process, this layer no longer protected the bulk from oxidation. These results were, thus, consistent with those obtained by other researchers [40-42].

According to Figure 10, the oxides layer's thickness was minimal and gradually grew for the Nd2 composite, as compared to the HfB_2-30 SiC composite. Furthermore, the oxide layer thickness in the HfB_2-based composites was less than the stated values in the previous research [43]. As a result of the rare earth oxide presence, the viscosity of the borosilicate glass layer was increased; due to the rise of the capillary forces, the borosilicate layer did not move directly to the upper surface, thus resulting in a more uniform mixture between the glass and oxide phases and improving the oxidation resistance of the UHTCs composite [32]. Therefore, by adding Nd_2O_3, the oxidation resistance of the HfB_2-30 SiC composite was improved, leading to the formation of a thinner oxide layer in this study.

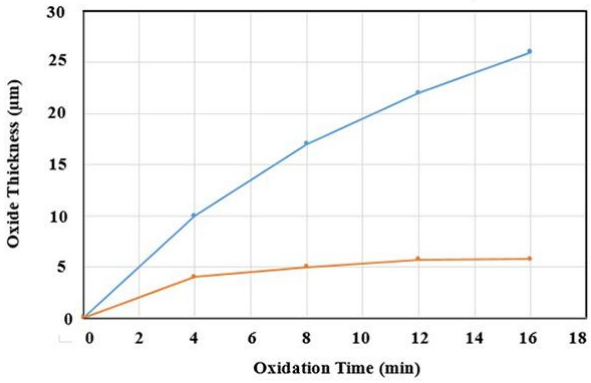

Figure 10. Variation of oxide layer thickness as a function of oxidation time for (a) HfB_2-SiC and (b) HfB_2-SiC-2 vol. % Nd_2O_3 composite

Figure 11 represents the weight gain with oxidation time for HfB_2-30 SiC and Nd2 composites following a 16 h oxidation test at a temperature of 1400 °C. The findings demonstrate that the Nd2 composite had substantially better oxidation resistance at this temperature due to the lower weight growth. The change of weight gain per unit surface area (W/S) as a function of oxidation time could determine the oxidation mechanism. The kinetic variables, n and k, could be obtained using Equation 6 [41]:

$$(\Delta W/S)^n = kt + B \quad (6)$$

where k is the constant of parabolic oxidation rate ($g^2cm^{-4}s^{-1}$), ΔW indicates the weight gain (g), S reflects the surface area (cm^2), t stands for the duration of isothermal oxidation (s), n represents the index of oxidation law ($0.35 \leq n \leq 0.55$ for parabolic behavior), and B is a constant.

A linear trend indicates response rate-controlled kinetics, while a parabolic one reflects diffusion rate-controlled ones. In the current research study, Nd2 exhibited a parabolic behavior (n = 0.51), while HfB_2-30 SiC had a linear one (n = 0.85) following the oxidation process for a period of 16 h at a temperature of 1400 °C. The HfB_2-30 SiC composite had low densification; therefore, the SiO_2 layer was generated locally on the composite surface. Thus, more oxygen penetrated the bulk owing to the active SiC oxidation at a high temperature of 1400 °C and more SiO (g) was formed, as compared to SiO_2 (l) (reaction (7)) [36], thus suggesting the oxidation control under this condition by the reaction rate.

$$SiC\ (s) + O_2\ (g) = SiO\ (g) + CO\ (g) \quad (7)$$

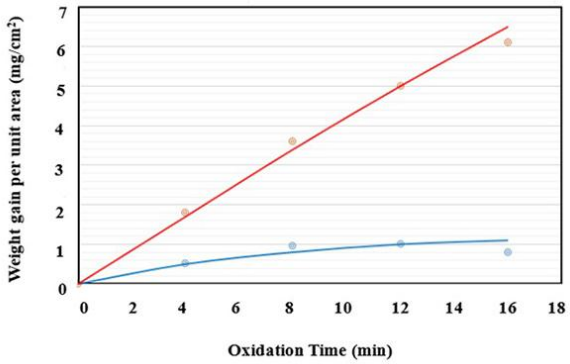

Figure 11. Weight gain as a function of oxidation time for (a) HfB_2-SiC and (b) HfB_2-SiC-2 vol. % Nd_2O_3 composite

The improved oxidation resistance of Nd2 composite could be associated to the generation of thin, dense, adherent, and protective layers formed as a result of the formed Si-based phase, thus leading to parabolic oxidation kinetics. These oxide layers can serve as barriers to the oxygen transport. Further, in the Nd2 composite, due to the generated oxycarbide compounds in the oxide layer and the decrease of oxygen diffusion, oxidation was controlled by the diffusion rate. However, following the formation of Nd-HfO_xC_y and Nd-SiO_xC_y phases, oxygen was applied at these phases of oxidation. Thus, the oxygen diffiusion rate in the bulk was reduced, hence improving the oxidation resistance of the composite and gradually increasing the oxidation rate in the incorporated HfB_2-30 SiC matrix. It is important to

note that the narrow, dense and compact layers comprising the Si-glass phase acted as a protective layer for the composite throughout the oxidation process, thus improving its oxidation resistance at high temperatures.

The Nd2 composite cross-section with high magnification can be seen in Figure 12.

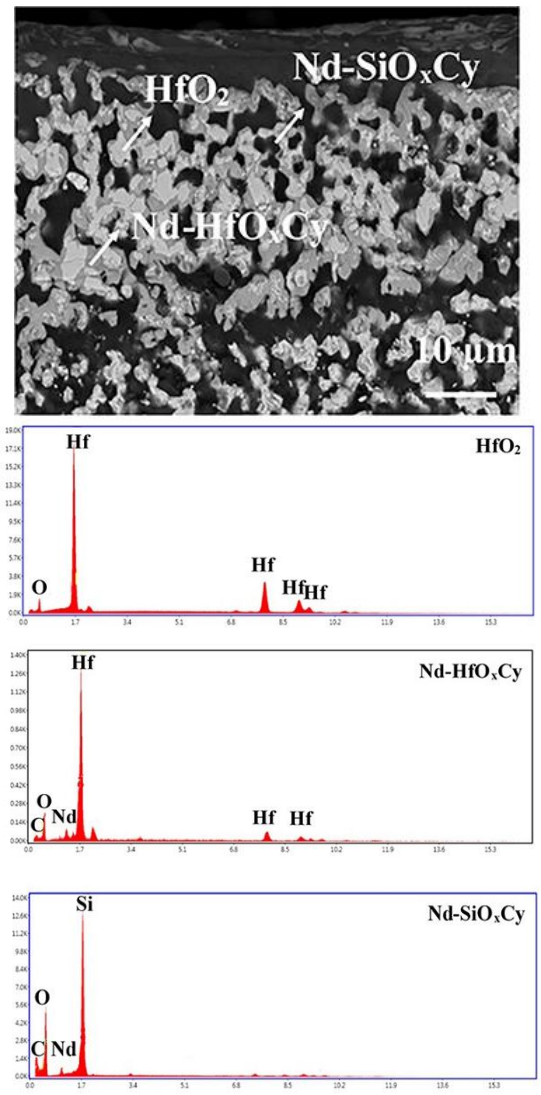

Figure 12. Cross-section of the HfB_2-SiC-2 vol. % Nd_2O_3 composite sample after the oxidation test for 16 h

Zapata et al. [32] found that with the addition of La_2O_3 to MeB_2 (Me = Hf, Zr)-SiC composites MeO_xC_y, La-MeO_xC_y and SiO_xC_y compounds formed following oxidation at 1500 °C for a period of 3 h, respectively. These researchers introduced the formed phases as new protective coatings for ultra-high temperature ceramics, as the oxygen diffusion coefficients were decreased and the oxidation resistance of the composites was raised to resist oxidation conditions for a long time. Thus, in this research study, the addition of Nd_2O_3 to HfB_2-SiC composites probably led to the formation of HfO_2, Nd-HfO_xC_y, and Nd-SiO_xC_y oxycarbide compounds in the oxide layer; thus, these compounds continuously reacted with oxygen and oxidized, reducing the penetration of oxygen-containing species into the composite. Therefore, the composite would follow a stabilized trend at long exposure times.

4. CONCLUSION

HfB_2-30 vol. % SiC and HfB_2-30 vol. % SiC-2 vol. % Nd_2O_3 composite samples were oxidized for 16 hours in a typical oxidation furnace to compare the oxidation behavior at a temperature of 1400 °C. Two layers were generated in each composite. The Si-based glass phase was in all layers. Based on microstructural examinations, no Si-depleted layer was discovered. After the oxidation procedure, a SiO_2 layer was generated on the surface of the oxidized HfB_2-30 vol. % SiC composite locally. This layer was extremely dense. The thickness of SiO_2 layer was calculated to be around 25 µm. Because of its increased porosity, the HfB_2-30 vol. % SiC composite indicated poor oxidation resistance, based on the findings. The thickness measurements revealed that the SiO_2 generated layer on the surface of Nd2 was 5 µm thick. After a 16-hour oxidation procedure at 1400 °C, Nd2 exhibited a parabolic behavior, while HfB_2-30 SiC exhibited a linear one. The improved oxidation resistance of this composite could be attributed to the formed Si-based phase and the decreased porosity, generating narrow, dense, adherent, and protective layers.

ACKNOWLEDGEMENTS

The authors wish to acknowledge Sharood University of Technology for the all support throughout this work.

REFERENCES

1. Chen, X., Feng, Q., Zhou, H., “Ablation behavior of three-dimensional C_f/SiC-ZrC-ZrB_2 composites prepared by a joint process of sol-gel and reactive melt infiltration”, ***Corrosion Science***, Vol. 134, (2018), 49-56. https://doi.org/10.1016/j.corsci.2018.02.011
2. Liu, T., Niu, Y., Li, C., Zhao, J., Zhang, J., Zeng, Y., Zheng, X., Ding, C., “Effect of $MoSi_2$ addition on ablation behavior of ZrC coating fabricated by vacuum plasma spray”, ***Ceramics International***, Vol. 44, No. 8, (2018), 8946-8954. https://doi.org/10.1016/j.ceramint.2018.02.093
3. Shojaie-Bahaabad, M., Hasani-Arefi, A., “Ablation properties of ZrC-SiC-HfB_2 ceramic with different amount of carbon fiber under an oxyacetylene flame”, Materials Research Express, Vol. 7, No. 2, (2020), 025604. https://doi.org/10.1088/2053-1591/ab70db
4. Binner, J., Porter, M., Baker, B., Zou, J., Venkatachalam, V., Diaz, V. R., D'Angio, A., Ramanujam, P., Zhang, T., Murthy, T. S. R. C., “Selection, processing, properties and

applications of ultra-high temperature ceramic matrix composites, UHTCMCs–a review", ***International Materials Reviews***, Vol. 65, No. 7, (2020), 389-444. https://doi.org/10.1080/09506608.2019.1652006

5. Ghelich, R., Jahannama, M. R., Abdizadeh, H., Torknik, F. S., Vaezi, M. R., "Hafnium diboride nonwoven mats with porosity/morphology tuned via different heat treatments", ***Materials Chemistry and Physics***, Vol. 248, (2020), 122876. https://doi.org/10.1016/j.matchemphys.2020.122876
6. Wang, H., Lee, S. H., Kim, H. D., Oh, H. C., "Synthesis of ultrafine hafnium diboride powders using solution-based processing and spark plasma sintering", ***International Journal of Applied Ceramic Technology***, Vol. 11, No. 2, (2014), 359-363. https://doi.org/10.1111/ijac.12016
7. Zou, J., Zhang, G. J., Kan, Y. M., Ohji, T., "Pressureless sintering mechanisms and mechanical properties of hafnium diboride ceramics with pre-sintering heat treatment", ***Scripta Materialia***, Vol. 62, No. 3, (2010), 159-162. https://doi.org/10.1016/j.scriptamat.2009.10.014
8. Monteverde, F., "Hot pressing of hafnium diboride aided by different sinter additives", ***Journal of Materials Science***, Vol. 43, No. 3, (2008), 1002-1007. https://doi.org/10.1007/s10853-007-2247-9
9. Ni, D. W., Liu, J. X., Zhang, G. J., "Pressureless sintering of HfB_2-SiC ceramics doped with WC", ***Journal of the European Ceramic Society***, Vol. 32, No. 13, (2012), 3627-3635. https://doi.org/10.1016/j.jeurceramsoc.2012.05.001
10. Gasch, M., Johnson, S., "Physical characterization and arc jet oxidation of hafnium based ultra-high temperature ceramics fabricated by hot pressing and field-assisted sintering", ***Journal of the European Ceramic Society***, Vol. 30, No. 11, (2010), 2337-2344. https://doi.org/10.1016/j.jeurceramsoc.2010.04.019
11. Ghadami, S., Taheri-Nassaj, E., Baharvandi, H. R., "Novel HfB_2-SiC-$MoSi_2$ composites by reactive spark plasma sintering", ***Journal of Alloys and Compounds***, Vol. 809, (2019), 151705. https://doi.org/10.1016/j.jallcom.2019.151705
12. Wang, H., Lee, S. H., Feng, L., "HfB_2-SiC composite prepared by reactive spark plasma sintering", ***Ceramics International***, Vol. 40, No. 7, (2014), 11009-11013. https://doi.org/10.1016/j.ceramint.2014.03.107
13. Ghadami, S., Taheri-Nassaj, E., Baharvandi, H. R., Ghadami, F., "Improvement of mechanical properties of HfB_2-based composites by incorporating in situ SiC reinforcement through pressureless sintering", ***Scientific Reports***, Vol. 11, No. 1, (2021), 1-11. https://doi.org/10.1038/s41598-021-88566-0
14. Zapata-Solvas, E., Jayaseelan, D. D., Lin, H. T., Brown, P., Lee, W. E., "Mechanical properties of ZrB_2-and HfB_2-based ultra-high temperature ceramics fabricated by spark plasma sintering", ***Journal of European Ceramic Society***, Vol. 33, No. 7, (2013), 1373-1386. https://doi.org/10.1016/j.jeurceramsoc.2012.12.009
15. Shahriari, M., Zakeri, M., Razavi, M., Rahimipour, M. R., "Investigation on microstructure and mechanical properties of HfB_2-SiC-HfC ternary system with different HfC content prepared by spark plasma sintering", ***International Journal of Refractory Metals and Hard Materials***, Vol. 93, (2020), 105350. https://doi.org/10.1016/j.ijrmhm.2020.105350
16. Mashayekh, S., Baharvandi, H. R., "Effects of SiC or $MoSi_2$ second phase on the oxide layers structureof HfB_2-based composites", ***Ceramics International***, Vol. 43, No. 17, (2017), 15053-15059. https://doi.org/10.1016/j.ceramint.2017.08.031
17. Guérineau, V., Vilmart, G., Dorval, N., Julian-Jankowiak, A. "Comparison of ZrB_2-SiC, HfB_2-SiC and HfB_2-SiC-Y_2O_3 oxidation mechanisms in air using LIF of $BO_2(g)$", ***Corrosion Science***, Vol. 163, (2020), 108278. https://doi.org/10.1016/j.corsci.2019.108278
18. Ghadami, S., Taheri-Nassaj, E., Baharvandi, H. R., Ghadami, F., "Effect of in situ VSi_2 and SiC phases on the sintering behavior and the mechanical properties of HfB_2-based composites", ***Scientific Reports***, Vol. 10, No. 1, (2020), 16540. https://doi.org/10.1038/s41598-020-73295-7
19. Simonenko, E. P., Simonenko, N. P., Lysenkov, A. S., Sevast'yanov, V. G., Kuznetsov, N. T., "Reactive Hot Pressing of HfB_2–SiC–Ta_4HfC_5 Ultra-High Temperature Ceramics", ***Russian Journal of Inorganic Chemistry***, Vol. 65, No. 3, (2020), 446-457. https://doi.org/10.1134/S0036023620030146
20. Simonenko, E. P., Simonenko, N. P., Nagornov, I. A., Sevastyanov, V. G., Kuznetsov, N. T., "Production and oxidation resistance of HfB_2–30 vol% SiC composite powders modified with $Y_3Al_5O_{12}$", ***Russian Journal of Inorganic Chemistry***, Vol. 65, No. 9, (2020), 1416-1423. https://doi.org/10.1134/S003602362009020X
21. Carney, C. M., "Oxidation resistance of hafnium diboride–silicon carbide from 1400 to 2000 ℃", ***Journal of Materials Science***, Vol. 44, No. 20, (2009), 5673-5681. https://doi.org/10.1007/s10853-009-3799-7
22. Carney. C. M, Parthasarathy, T. A., Cinibulk, M. K., "Oxidation resistance of hafnium diboride ceramics with additions of silicon carbide and tungsten boride or tungsten carbide", ***Journal of the American Ceramic Society***, Vol. 94, No. 8, (2011), 2600-2607. https://doi.org/10.1111/j.1551-2916.2011.04462.x
23. Guo, S., "Oxidation and strength retention of HfB_2−SiC composite with La_2O_3 additives", ***Advances in Applied Ceramics***, Vol. 119, No. 4, (2020), 218-223. https://doi.org/10.1080/17436753.2020.1755510
24. Sciti, D., Balbo, A., Bellosi, A., "Oxidation behavior of a pressureless sintered HfB_2–$MoSi_2$ composite", ***Journal of the European Ceramic Society***, Vol. 29, No. 9, (2009), 1809-1815. https://doi.org/10.1016/j.jeurceramsoc.2008.09.018
25. Opila, E., Levine, S., Lorincz, J., "Oxidation of ZrB_2- and HfB_2-based ultra-high temperature ceramics: Effect of Ta conditions", ***Journal of Materials Science***, Vol. 39, No. 19, (2004), 5969-5977. https://doi.org/10.1023/B:JMSC.0000041693.32531.d1
26. Simonenko, E. P., Simonenko, N. P., Gordeev, A. N., Kolesnikov, A. F., Chaplygin, A. V., Lysenkov, A. S., Nagornov, I. A., Sevastyanov, V. G., Kuznetsov, N. T., "Oxidation of HfB_2-SiC-Ta_4HfC_5 ceramic material by a supersonic flow of dissociated air", ***Journal of the European Ceramic Society***, Vol. 41, No. 2, (2021), 1088-1098. https://doi.org/10.1016/j.jeurceramsoc.2020.10.001
27. Bannykh, D., Utkin, A., Baklanova, N., "Effect of chromium additive on sintering and oxidation behavior of HfB2-SiC ceramics", ***Ceramics International***, Vol. 44, No. 11, (2018), 12451-12457. https://doi.org/10.1016/j.ceramint.2018.04.035
28. Kováčová, Z., Bača, Ľ., Neubauer, E., Kitzmantel, M., "Influence of sintering temperature, SiC particle size and Y_2O_3 addition on the densification, microstructure and oxidation resistance of ZrB_2–SiC ceramics", ***Journal of the European Ceramic Society***, Vol. 36, No. 12, (2016), 3041-3049. https://doi.org/10.1016/j.jeurceramsoc.2015.12.028
29. Guo, W. M., Vleugels, J., Zhang, G. J., Wang, P. L., Van der Biest, O., "Effects of Re_2O_3 (Re = La, Nd, Y and Yb) addition in hot-pressed ZrB_2–SiC ceramics", ***Journal of the European Ceramic Society***, Vol. 29, No. 14, (2009), 3063-3068. https://doi.org/10.1016/j.jeurceramsoc.2009.04.021
30. Ren, X., Mo, H., Wang, W., Feng, P., Guo, L., Li, Z., "Ultrahigh temperature ceramic HfB_2-SiC coating by liquid phase sintering method to protect carbon materials from oxidation", ***Materials Chemistry and Physics***, Vol. 217, (2018), 504-512. https://doi.org/10.1016/j.matchemphys.2018.07.018
31. Wang, P., Li, H., Yuan, R., Wang, H., Zhang, Y., Zhao, Z., "The oxidation resistance of two-temperature synthetic HfB_2-SiC coating for the SiC coated C/C composites", ***Journal of Alloys and Compounds***, Vol. 747, (2018), 438-446. https://doi.org/10.1016/j.jallcom.2018.03.043
32. Zapata-Solvas, E., Jayaseelan, D. D., Brown, P. M., Lee, W. E., "Effect of La_2O_3 addition on long-term oxidation kinetics of ZrB_2–SiC and HfB_2-SiC ultra high temperature ceramics", ***Journal of the***

European Ceramic Society, Vol. 34, Vol. 15, (2014), 3535-3548. https://doi.org/10.1016/j.jeurceramsoc.2014.06.004

33. Duran. P, "Phase relationships in the systems HfO_2-La_2O_3 and HfO_2-Nd_2O_3", ***Ceramics International***, Vol. 1, No. 1, (1975), 10-13. https://doi.org/10.1016/0390-5519(75)90032-0
34. Sevastyanov, V. G., Simonenko, E. P., Sevastyanov, D. V., Simonenko, N. P., Stolyarova, V. L., Lopatin, S. I., Kuznetsov, N. T., "Synthesis, vaporization and thermodynamics of ultrafine $Nd_2Hf_2O_7$ powders", ***Russian Journal of Inorganic Chemistry***, Vol. 58, No. 1, (2013), 1-8. https://doi.org/10.1134/S0036023613010178
35. Jaberi Zamharir, M., Shahedi Asl, M., Pourmohammadie Vafa, N., Ghassemi Kakroudi, M., "Significance of hot pressing parameters and reinforcement size on densification behavior of ZrB_2-25 vol% SiC UHTCs", ***Ceramics International***, Vol. 41, No. 5, (2015), 6439-6447. https://doi.org/10.1016/j.ceramint.2015.01.082
36. Ghadami, S., Taheri-Nassaj, E., Baharvandi, H. R., Ghadami, F., "Effect of in situ SiC and $MoSi_2$ phases on the oxidation behavior of HfB_2- based composites", ***Ceramics International***, Vol. 46, No. 12, (2020), 20299-20305. https://doi.org/10.1016/j.ceramint.2020.05.116
37. Vinci, A., Zoli, L., Galizia, P., Sciti, D., "Influence of Y_2O_3 addition on the mechanical and oxidation behavior of carbon fiber reinforced ZrB_2/SiC composites", ***Journal of the European Ceramic Society***, Vol. 40, No. 15, (2020), 5067-5075. https://doi.org/10.1016/j.jeurceramsoc.2020.06.043
38. Wang, P., Li, H., Sun, J., Yuan, R., Zhang, L., Zhang, Y., Li, T., "The effect of HfB_2 content on the oxidation and thermal shock resistance of SiC coating", ***Surface and Coatings Technology***, Vol. 339, (2018), 124-131. https://doi.org/10.1016/j.surfcoat.2018.02.029
39. Jin, H., Meng, S., Zhang, X., Zeng, Q., Niu, J., "Effects of oxidation temperature, time, and ambient pressure on the oxidation of ZrB_2–SiC–graphite composites in atomic oxygen", ***Journal of the European Ceramic Society***, Vol. 36, No. 8, (2016), 1855-1861. https://doi.org/10.1016/j.jeurceramsoc.2016.02.040
40. Parthasarathy, T. A., Rapp, R. A., Opeka, M., Kerans, R. J., "A model for the oxidation of ZrB_2, HfB_2 and TiB_2", ***Acta Materialia***, Vol. 55, No. 17, (2007), 5999-6010. https://doi.org/10.1016/j.actamat.2007.07.027
41. Mallik, M., Ray, K. K., Mitra, R., "Oxidation behavior of hot pressed ZrB_2–SiC and HfB_2–SiC composites", ***Journal of the European Ceramic Society***, Vol. 31, No. 1-2, (2011), 199-215. https://doi.org/10.1016/j.jeurceramsoc.2010.08.018
42. Lespade, P., Richet, N., Goursat, P., "Oxidation resistance of HfB_2–SiC composites for protection of carbon-based materials", ***Acta Astronautica***, Vol. 60, No. 10-11, (2007), 858-864. https://doi.org/10.1016/j.actaastro.2006.11.007
43. Ghadami, F., Aghdam, A. S. R., Zakeri, A., Saeedi, B., Tahvili, P., "Synergistic effect of CeO_2 and Al_2O_3 nanoparticle dispersion on the oxidation behavior of MCrAlY coatings deposited by HVOF", ***Ceramics International***, Vol. 46, No. 4, (2020), 4556-4567. https://doi.org/10.1016/j.ceramint.2019.10.184